The TESS Full Orbital Phase Curve and Gravity Darkening Analysis of KELT-9 System.

Patcharapol Wachiraphan

Department of Physics

Mahidol University

Supervisor

Petchara Pattarakijwanich Ph.D.

In partial fulfillment of the requirements for the degree of

Bachelor of Science in Physics

June 1, 2020

Acknowledgements

I would like to express the deepest appreciation to my supervisor Dr. Petchara Pattarakijwanich for advice and the opportunity to work in astrophysics, especially in the exoplanet field. And, also Dr. George Zhou and Dr. Chelsea X. Huang for support in academic knowledge, skills, and the concept of this research during summer research 2019 at the Harvard-Smithsonian Center for Astrophysics (CfA) and the MIT Kavli Institute for Astrophysics and Space Research at Cambridge, Massachusetts, United States of America.

I would like to thank people in the Department of Physics, Faculty of Science, Mahidol University, especially administrative officers, to help me in detail paperwork during all courses.

In addition, a thank you to Prof. Dr.David Ruffolo and Asst. Prof. Dr. Warit Mitthumsiri for support in high performance computing cluster at Space and Astrophysics Lab, Department of Physics, Faculty of Science, Mahidol University.

Finally, I would like to thank Sri-Tang-Tong scholarship for funding and the opportunity to do summer research aboard.

Abstract

KELT-9b is an ultra-hot Jupiter discovered by Gaudi et al. (2017) orbiting around a rapid-rotator oblate KELT-9 star. In this research, we aim to fit gravity-darkened transit, phase curve variation, and global parameters of the KELT-9 system using TESS photometric data, TRES spectroscopic data and avialable apparent magnitudes in many filters. Our fitting model takes into account asymmetric transit (*simutrans*, Herman et al. (2018)), spectroscopic Doppler tomography, and isochrone fitting. After running MCMC (*emcee*, Foreman-Mackey et al. (2013)) through the model, we got stellar inclination $I_{rot} = 58.67\ ^{+0.88}_{-0.34}$ degree and sky-projected spin-orbit misalignment angle (λ) = 274.78 $\pm$ 0.25 degree which imply a nearly polar orbit. Moreover, we finally got $R_p/R_* = 0.079772\ ^{+0.000059}_{-0.000061}$ which is significantly lower than from Gaudi et al. (2017) as we expected, due to the gravity darkening effect on polar orbit transit. In term of phase curve variation, we adopt the model from Esteves et al. (2013) and got the amplitude of each term as follow, the amplitude of phase function term (A_p) = $498.7\ ^{+7.3}_{-8.0}$ ppm, the amplitude of doppler boosting term (A_d) = $44.9\ ^{+2.9}_{-2.8}$ ppm, the amplitude of ellipsoidal variation term (A_e) = $23.8\ ^{+4.0}_{-3.9}$ ppm, and secondary eclipse depth (f_p) = $637.2\ ^{+9.0}_{-8.9}$. These results are all self-consistent and fit together reasonably well. Finally, we need to emphasize the potential and importance of The Transiting Exoplanet Survey Satellite (TESS) to study gravity-darkened transit and phase curve variation to understand the physics behind these effects better.

Contents

List of Figures

List of Tables

Chapter 1

Introduction

In today's world, extra-solar planet or exoplanet is one of the most active research fields in astronomy and astrophysics. It mainly studies about formation, evolution, and atmosphere of planets outside our solar system to understand the nature of planets at least in our solar neighbourhood. Since the discovery of the first exoplanet orbiting around a main-sequence star, 51 Pegasi b (Mayor and Queloz, 1995), over 4000 exoplanets have been discovered in 25 years (NASA exoplanet archive, Retrieved April, 30, 2020). There are many methods of detecting and studying exoplanet such as radial velocity method, transit method, direct imaging method, microlensing method, etc. However, nearly 95% of them are discovered from the two most common techniques, which are radial velocity and transit method.

1.1 Rationale and Signification

Gravity darkening and phase curve variation effects affect the total brightness of the system at a part-per-thousand level, which cannot be observed in the past ground-based surveys. However, since we can observe from space, we are able to study these small scale effects accurately and should include them in the model. Transiting Exoplanet Survey Satellite (TESS) is the latest NASA's all-sky survey space telescope mainly looking for transiting exoplanets. Shporer et al. (2019) and Zhou et al. (2019) showed the potential of using TESS photometric data to study either phase curve variation and gravity darkening effect, respectively.

So, we expected to include these effects to the transit model and improve transit parameters of exoplanet system.

1.2 Objectives

This research will focus on building a transit model of phase curve variation, gravity darkening effect, isochrone fitting and global transit parameters and subsequently using Transiting Exoplanet Survey Satellite (TESS) photometric data, Tillinghast Reflector Echelle Spectrograph (TRES) spectroscopic data, and magnitudes in various filters on KELT-9 to constrain a set of model parameters.

1.3 Overview of the Report

This research report includes five chapters. The introduction, rationale and signification, and objective of this research are in chapter 1. Chapter 2 is about background knowledge and previous related work. Then, all methodology and the overall process will be presented in the chapter 3. The result and discussion are in chapter 4. Finally, chapter 5 is about the conclusion of this research.

Chapter 2

Background and Related Works

This research includes either photometric analysis that used photometric data from TESS and spectroscopic analysis that used spectroscopic data from TRES (Gaudi et al., 2017). The several advanced astronomic effects and analysis method related to this works will be provided in this chapter including observations and target [See 2.1], photometric analysis [See 2.2], and spectroscopic analysis [See 2.3] of exoplanet. We also include isochrone fitting analysis [See 2.4] for the star in this chapter.

2.1 Observations and Target

In this section, information about observation and target, which is used in this research is provided. The two observations used in this research are Transiting Exoplanet Survey Satellite (TESS), NASA's space telescope looking for transiting exoplanet, and Tillinghast Reflector Echelle Spectrograph (TRES), Smithsonian Astrophysical Observatory's Echelle spectrograph located at Mt. Hopkins in Arizona, USA. The target star of this research is KELT-9 star which has one confirmed ultra-hot Jupiter orbit around.

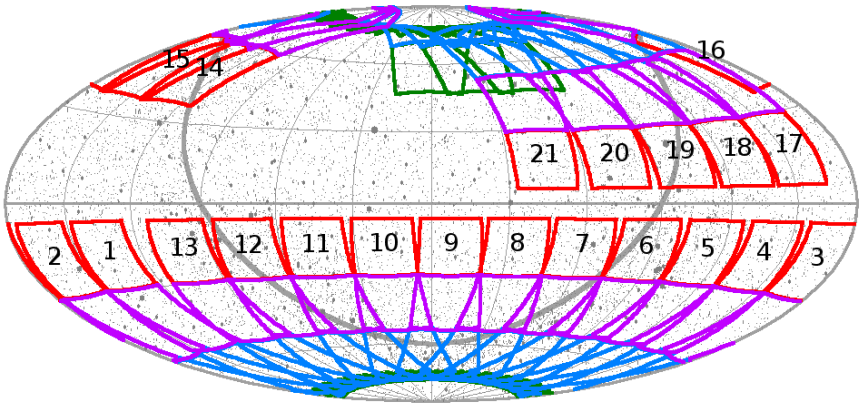

Figure 2.1 The illustration of TESS sky coverage map.

2.1.1 Observations

2.1.1.1 Transiting Exoplanet Survey Satellite (TESS)

The Transiting Exoplanet Survey Satellite (TESS) is NASA's space-based telescope launched on 18 April 2018, to replace the old Kepler space telescope. Unlike Kepler that was designed to look at the same direction for earth-size planets, TESS was designed to be an all-sky survey monitoring brightness of nearby stars with apparent magnitudes brighter than 12. In TESS two-years mission, the sky is divided into 26 observation sector.The sky coverage map is shown in Figure 2.1.

Each sector is observed by four cameras with Field of View (FoV) $24^\circ \times 24^\circ$ each, for 27 days. After 27 days of observing, the data will be downlinked and calibrated by the Science Processing and Operations Center (SPOC) team. Then, the data will be released at the Mikulski Archive for Space Telescopes (MAST) for the public.

In addition, TESS has two types of images: the 2-minutes cadence images and Full-Frame Images (FFIs). First, 2-minutes cadence images are the stack of 2-second data from cameras together to get better resolution. Targets of 2-minutes cadence images are pre-selected from the good planet candidates as Target of Interest (TOI). Second, Full-Frame Images (FFIs) are 30-minutes cadence image with bigger FoV than 2-minutes cadence and have less sensitivity.

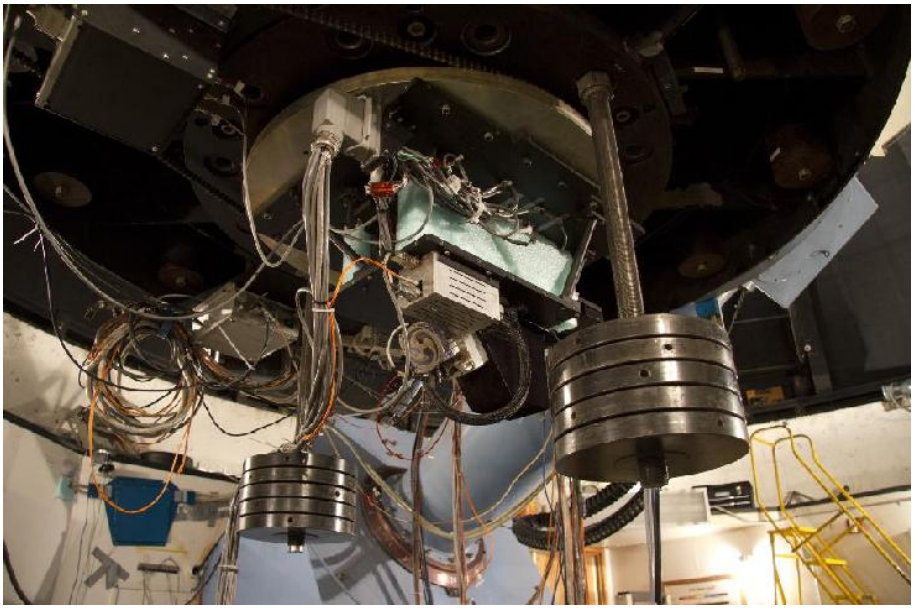

Figure 2.2 A view of the TRES head from the NE in the chamber (April 2014).

2.1.1.2 Tillinghast Reflector Echelle Spectrograph (TRES)

Tillinghast Reflector Echelle Spectrograph (TRES) is a fiber-fed cross-dispersed echelle spectrograph mounted in 1.5-m Tillinghast optical spectroscopic telescope, Fred Lawrence Whipple Observatory, Mt. Hopkins, Arizona, US. TRES has a wavelength range from 390 nm to 910 nm and offers three resolution at 60K, 48K, and 30K. The setup of TRES is shown in Figure 2.2.

2.1.2 Target (KELT-9)

KELT-9 or HD 195689 is an A0 type star with apparent magnitude 7.56 in V-band located around 615 light-years from solar systems in the constellation of Cygnus. KELT-9 has one known exoplanet orbit around. KELT-9b is an ultra-hot Jupiter with an orbital period of around 1.48 days. KELT-9b was discovered by Gaudi et al. (2017) during the Kilodegree Extremely Little Telescope (KELT) survey. Physical parameters of the star and planet from Gaudi et al. (2017) are shown in table 2.1.

Parameters	Value	Error
Orbital and transit parameters		
T_0 (BJD - 2457000)	95.68572	± 0.00014
P (d)	1.4811235	±0.0000011
R_p/R_*	0.08228	±0.00043
a/R_*	3.153	±0.0011
i_{orbit} (degree)	86.79	±0.25
f_p (ppm)	1006	±97
e	0.0 (fixed)	-
ω_*.....	90 (fixed)	-
Stellar parameters		
I_{rot} (degree)	-	-
λ (degree)	275.2	± 1.4
M_* ($M_\odot$)	2.52	$^{+0.25}_{-0.20}$
R_* ($R_\odot$)	2.362	$^{+0.075}_{-0.063}$
vsini (km/s)	111.4 (fixed)	-

Table 2.1: Gaudi et al. (2017) transit and stellar parameters.

2.2 Photometric Analysis

One of the most common exoplanet detection methods which discovered almost 77% of confirmed exoplanets these days is the transit method. The transit method uses only our capability of monitoring the brightness of the system. Because we can not resolve light from planets and stars separately, so we only measure the total flux of the system that includes various astronomical effects in consideration. Unfortunately, we can not include either phase curve variation [See 2.2.1] and gravity darkening [See 2.2.2] in our model in the past because of our big error. Now, when we can reduce the limit of the detection method to around 60 ppm, we can include the model of different astronomical effects that affect the total brightness of the system.

2.2.1 Phase curve variations

In this topic, we will consider the time-series of the brightness of the system called light curve. In the phase-folded light curve, we may notice wobble due to interactions between planets and stars call "phase curve variation". Esteves et al. (2013) has shown four physical components of phase curve variation: i) F_p, the planet phase function; ii) F_e, the ellipsoidal variations; iii) F_d, the doppler boosting

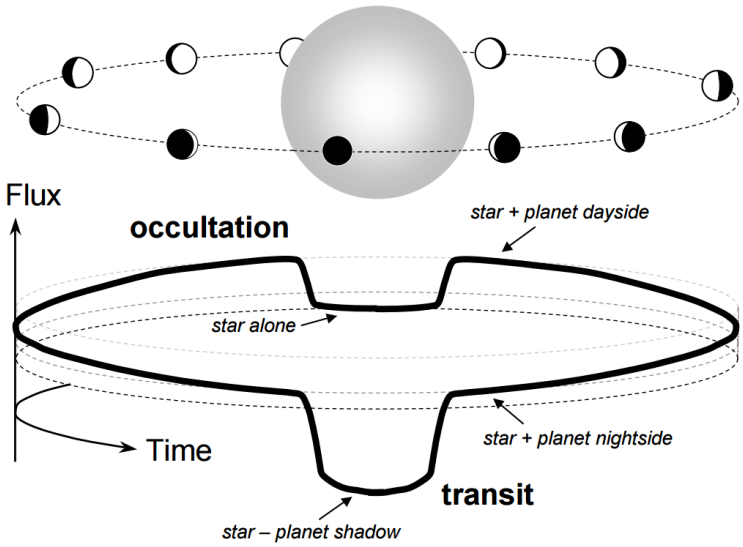

Figure 2.3 The illustrator of transit, secondary eclipse and phase function.

term; iv) F_{ecl}, secondary eclipse term which all of these terms are functions of phase of the planet (ϕ).

- **Planet phase function term (F_p).** This term is the planet's reflected light as a Lambert sphere (Russell, 1916). When the planet orbits around the star, we can observe the different amount of total light due to the planet's scatter light which varies as a function of orbital phase. This effect is the same effect as the moon's phase as in Figure 2.3.

  We can describe this term in equation 2.1.

$$F_p = A_p \frac{\sin(z) + (\pi - z)\cos(z)}{\pi} \tag{2.1}$$

  where A_p is the amplitude of the planet phase curve term, z is related to phase of planet (ϕ) and orbital inclination (i) as in equation 2.2.

$$\cos(z) = -\sin(i)\cos(2\pi\phi) \tag{2.2}$$

- **Doppler boosting term (F_d).**This term is the relativistic term due to light source moving toward or away from the observer. When the star is moving toward the observer, the observers can detect brighter intensity than when the star is moving away. For the obvious example, if we observe the AGN jets of the galaxies M87, we can only see the single jet as in Figure 2.4 because

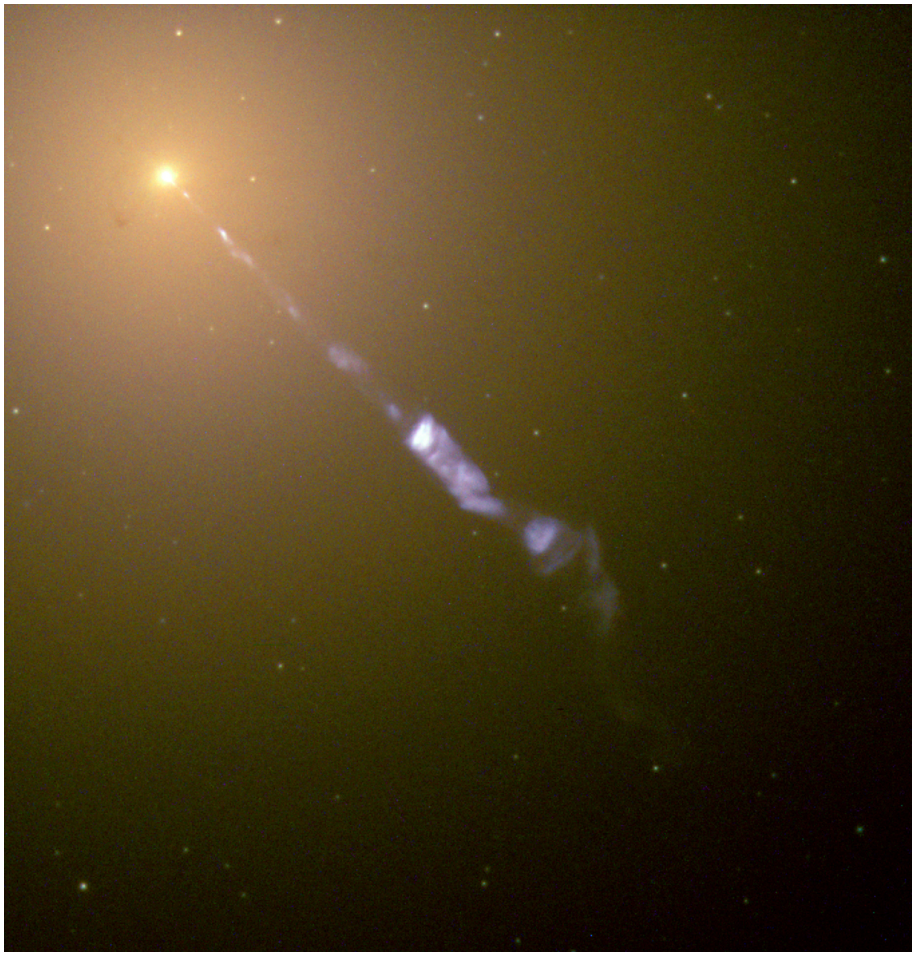

Figure 2.4 Only a single jet is visible in M87 from NASA and The Hubble Heritage Team (STScI/AURA).

of the Doppler boosting effect. For exoplanet light curve, this variation can be described in term of orbital phase (ϕ) as in equation 2.3.

$$F_d = A_d \sin(2\pi\phi) \tag{2.3}$$

where A_d is the amplitude of the doppler boosting term.

- **Ellipsoidal variations term (F_e)** is driven by tidal reaction between the planet and its host star. This reaction affects the host star shape from spherical to ellipsoidal that changes the total flux from the star along the planet's phase. This term can be written as a linear combination of the first three cosine harmonics of the planet's period (Morris, 1985) which can be

described as in equation 2.4.

$$F_e = -A_e[\cos(2\pi \cdot 2\phi) + f_1 \cos(2\pi\phi) + f_2 \cos(2\pi \cdot 3\phi)] \tag{2.4}$$

where A_e is the amplitude of the ellipsoidal variations term, f_1, f_2 are constant of the systems related to a/R$_*$ and orbital inclination (i) as in equation 2.5.

$$\begin{aligned} f_1 &= 3\alpha_1 \left(\frac{a}{R_*}\right)^{-1} \frac{5\sin^2(i) - 4}{\sin(i)} \\ f_2 &= 5\alpha_1 \left(\frac{a}{R_*}\right)^{-1} \sin(i) \end{aligned} \tag{2.5}$$

where α_1 can be described as equation 2.6.

$$\alpha_1 = \frac{25u}{24(15+u)} \left(\frac{y+2}{y+1}\right) \tag{2.6}$$

where u and y are linear and quadratic term of quadratic limb-darkening coefficient respectively.

- **Secondary Eclipse term (F_{ecl}).** This term occurs when the planet is behind the star in the line of sight. The total brightness of the system decrease as in equation 2.7 (Kreidberg, 2015)

$$F_{ecl} = 1 + f_p(1 - \alpha) \tag{2.7}$$

where f_p is the planet-to-star flux ratio. α is the fraction of the planet disk that is occulted by the star.

2.2.2 Gravity darkening

Albrecht et al. (2012) show that many hot-Jupiters, gas giant planets orbit in a close-in orbit, have a misalignment between planet orbital axis and star rotation axis. So, the study of spin-orbit misalignment of exoplanet and its host star can help our understanding of planet formation, migration, and evolution. The typical approach to study spin-orbit misalignment has been done through the Rossiter-

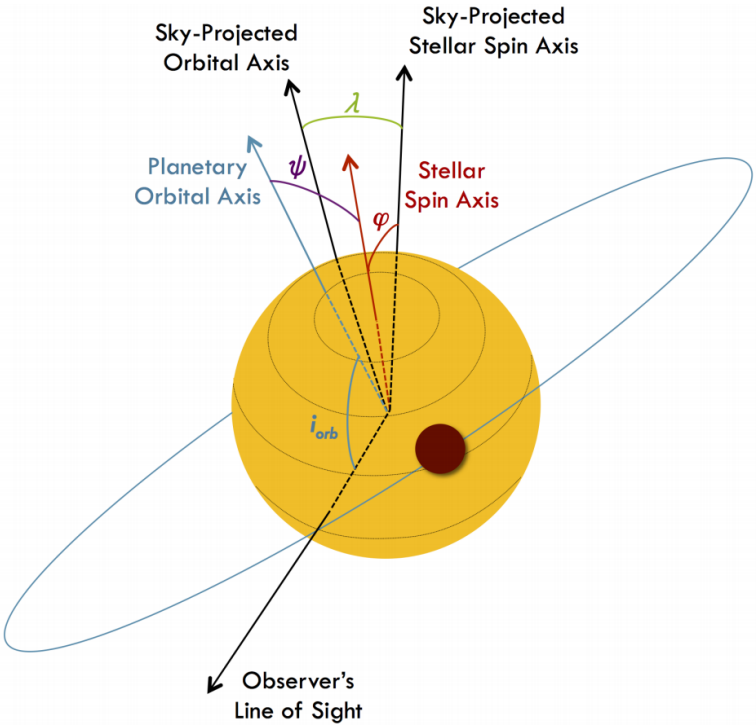

Figure 2.5 The illustrator of 3-D structure of planetary system from Herman et al. (2018).

McLaughlin (RM) effect [See 2.3.1], which using spectroscopic data of the system. However, using the RM effect is limited in two ways. First, The RM effect only provides the information on the sky-projected spin-orbit misalignment angle (λ) but not stellar rotation inclination (I_*) or orbital inclination (i_{orb}), so we can not construct the true-3D spin-orbit misalignment angle (ψ). Second, rapid-rotating star has a lack of many spectral lines that make using RM effect difficult.

Main-sequence stars early than spectral type ~F6 are expected to have high rotational velocity because of the radiative structure. These rapid-rotators are normally in oblate shape due to their high centrifugal force from rotational velocity and have high surface gravity (g) as described in Barnes (2009). von Zeipel (1924) also derived a relationship between surface gravity (g) and effective temperature (also related to stellar brightness) as in equation 2.8.

$$\frac{T}{T_{pole}} = \left(\frac{g}{g_{pole}}\right)^{\beta} \tag{2.8}$$

where β is gravity darkening exponent (Espinosa Lara and Rieutord, 2011).

So, if the planets misaligned from the star's rotation axis and we are in the

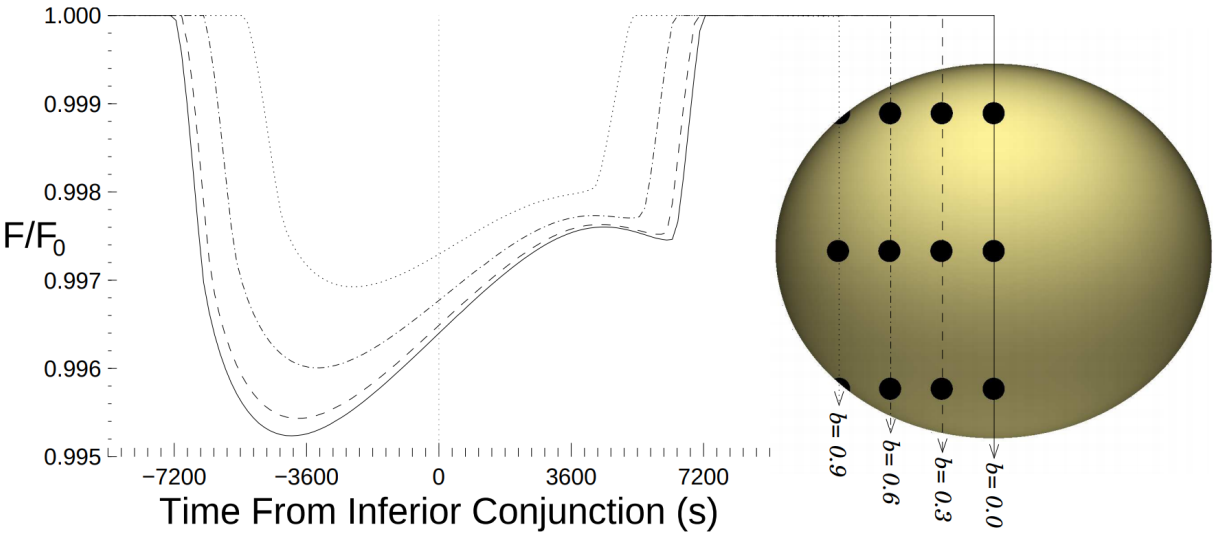

Figure 2.6 An example of asymmetric transit with different impact factor (b) from Barnes (2009).

line of sight to see the transit, we should be able to see an asymmetric transit because the planet's shadow conceals different amount of light through the path as in Figure 2.6. From this technique, we are able to constrain either λ and I_*.

However, the only two planets confirmed with this asymmetric gravity darkened transits are *Kepler*-13 (Szabó et al. (2011), Barnes et al. (2011), and Herman et al. (2018)) and *HAT-P*-70 (Zhou et al., 2019) because this effect will only affect in part-per-thousand scale.

2.3 Spectroscopic Analysis

Spectroscopy always is the best way to extract information for astrophysics since they contain information about the dynamic, composition, and interaction of celestial objects. However, we can use spectroscopy to implement a different technique to extract different information. The most common and important technique for exoplanet detection is doppler spectroscopy. Doppler spectroscopy or radial-velocity method observes the doppler shift of the stellar spectrum. On the other hand, if we are observing an in-transit situation, we can cobtain more information on planet's atmospheric composition and also sky-projected spin-orbit misalignment angle (λ) via the Rossiter–McLaughlin effect [See 2.3.1].

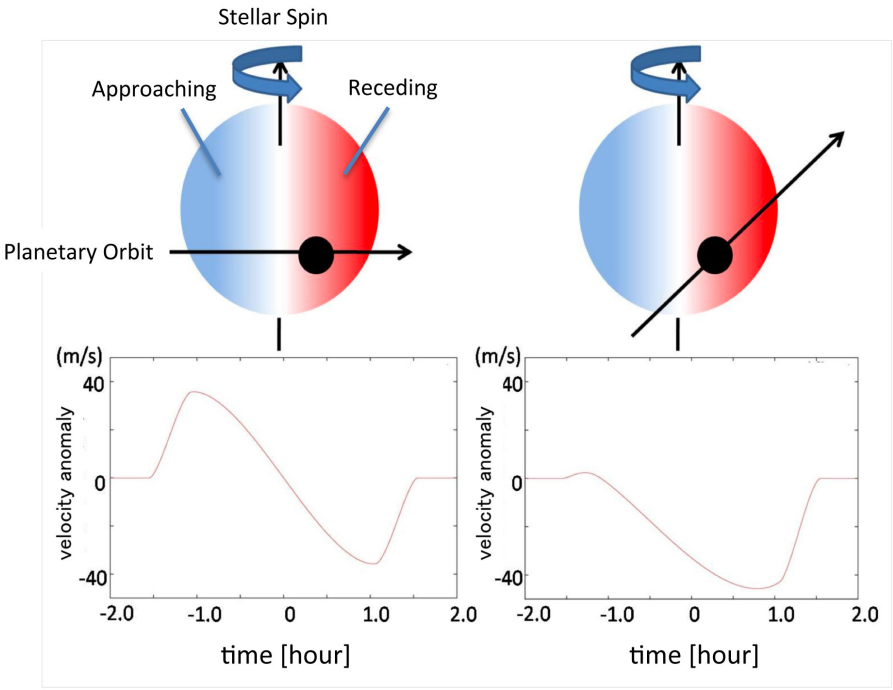

Figure 2.7 Schematic Diagram of the Rossiter-McLaughlin (RM) Effect.

2.3.1 Rossiter–McLaughlin effect

The Rossiter–McLaughlin effect (Rossiter (1924) and McLaughlin (1924)) is a spectroscopic phenomenon that occurs when an object transit across a rotating star. From the spectrum of the star, we expect a certain rotational velocity (v_{rot}) from the doppler effect over time. Nevertheless, when there is an object move across different parts of the star with different λ, it will create a different pattern of v_{rot} distortion, as shown in Figure 2.7.

2.4 Isochrone analysis

Isochrone fitting is the technique that is used to infer the physical parameters of stars. An isochrone is a same-age line in the Hertzsprung-Russell (HR) diagram, calculated from the stellar evolution model at different initial mass, metallicity, and some other physical parameters. With the isochrone grid, which is a set of stellar evolution track, we can interpolate our isochrone grid to fit for stellar parameters based on observational data.

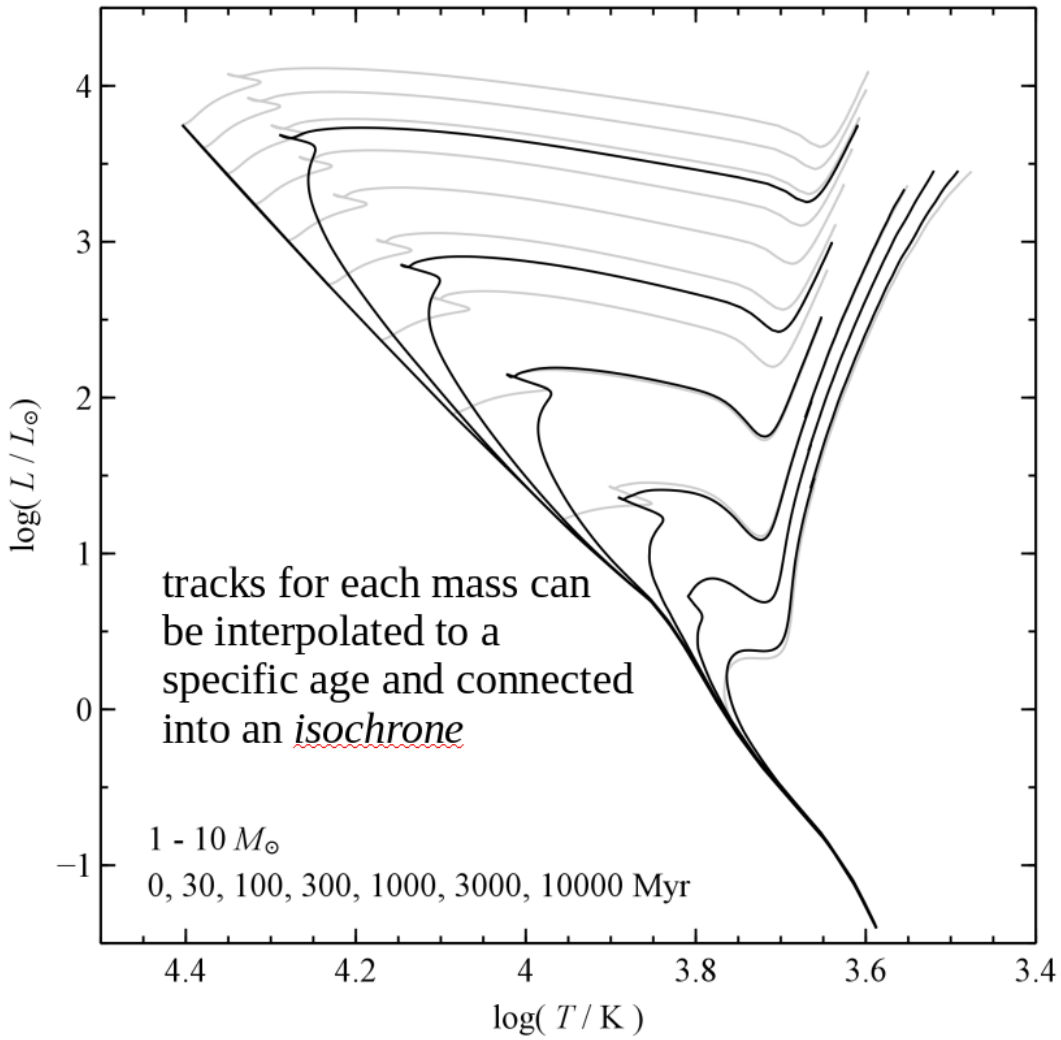

Figure 2.8 HR diagram of Evolutionary tracks for stars with masses from 1 to 10 $M_\odot$(Grey) and interpolated tracks at fixed ages (Black).

Chapter 3

Methodology

This chapter describes the process of this research, starting from data preparation [See 3.1], model creation [See 3.2], and analysis calculation [See 3.3]. Diagram showing overall process is showed in Figure 3.1.

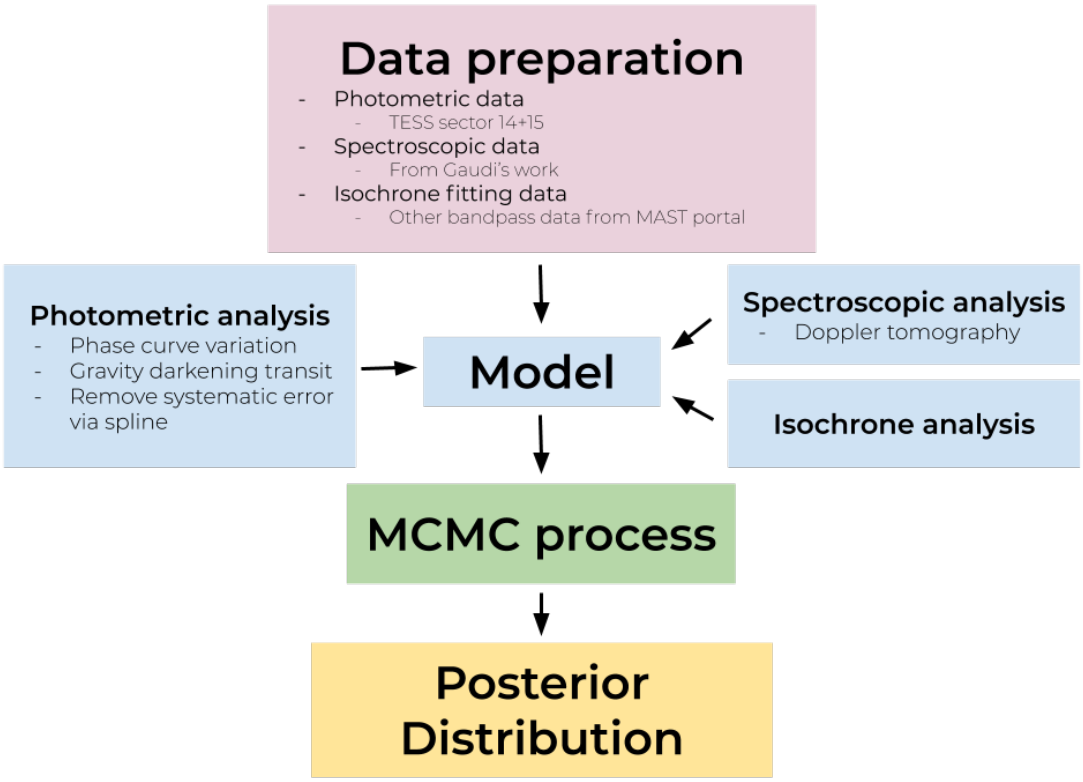

Figure 3.1 Diagram of overall process.

3.1 Data Preparation

3.1.1 Photometric data

In this research, we used TESS photometric data of KELT-9 (TIC 16740101) downloaded from the Mikulski Archive for Space Telescopes (MAST) portal, as shown in Figure 3.2.

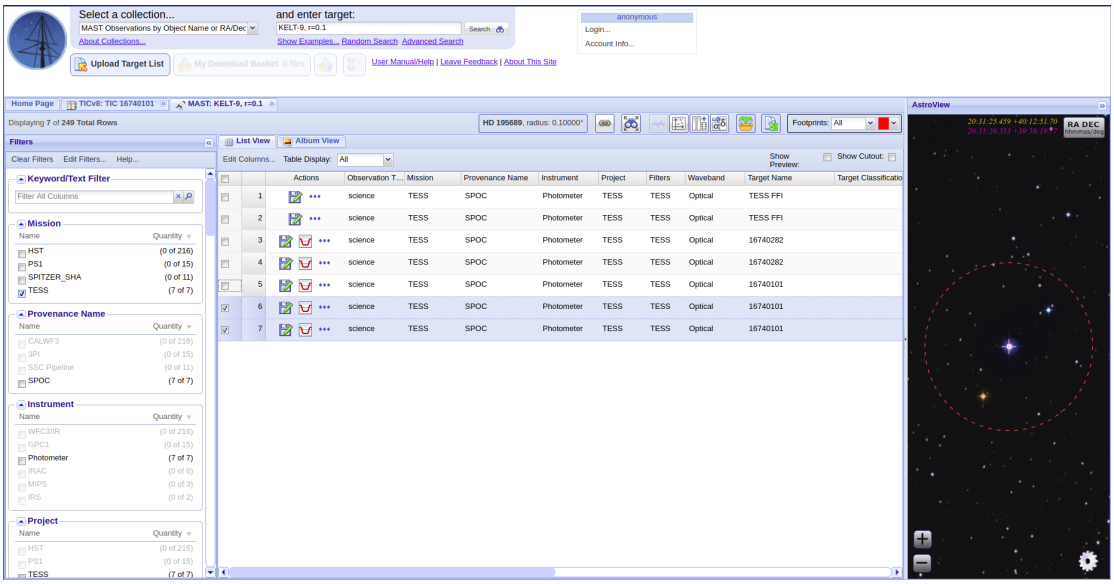

Figure 3.2 MAST portal for TESS KELT-9 data.

In the FITS file we downloaded, we used the Presearch Data Conditioning Simple Aperture Photometry (PDCSAP) light curve, which removed the systematic error (Smith et al., 2012; Stumpe, Smith, Van Cleve, et al., 2012; Stumpe, Smith, Catanzarite, et al., 2014) in our photometric analysis. We provided SAP and PDCSAP light curve in Figure 3.3.

Then, we masked out points that are NaN and bad quality points according to the quality flag that was provided by SPOC (Jenkins et al., 2016). We also masked out the outlying data points that may occur due to flare or systematic error from the starting of orbit 38 (BJD 2458724.93585) to BJD 2458725.94321225. After that, the PDCSAP flux and PDCSAP flux error were divided by median flux in order to normalized flux to unity. We show the prepared light curve in Figure 3.4.

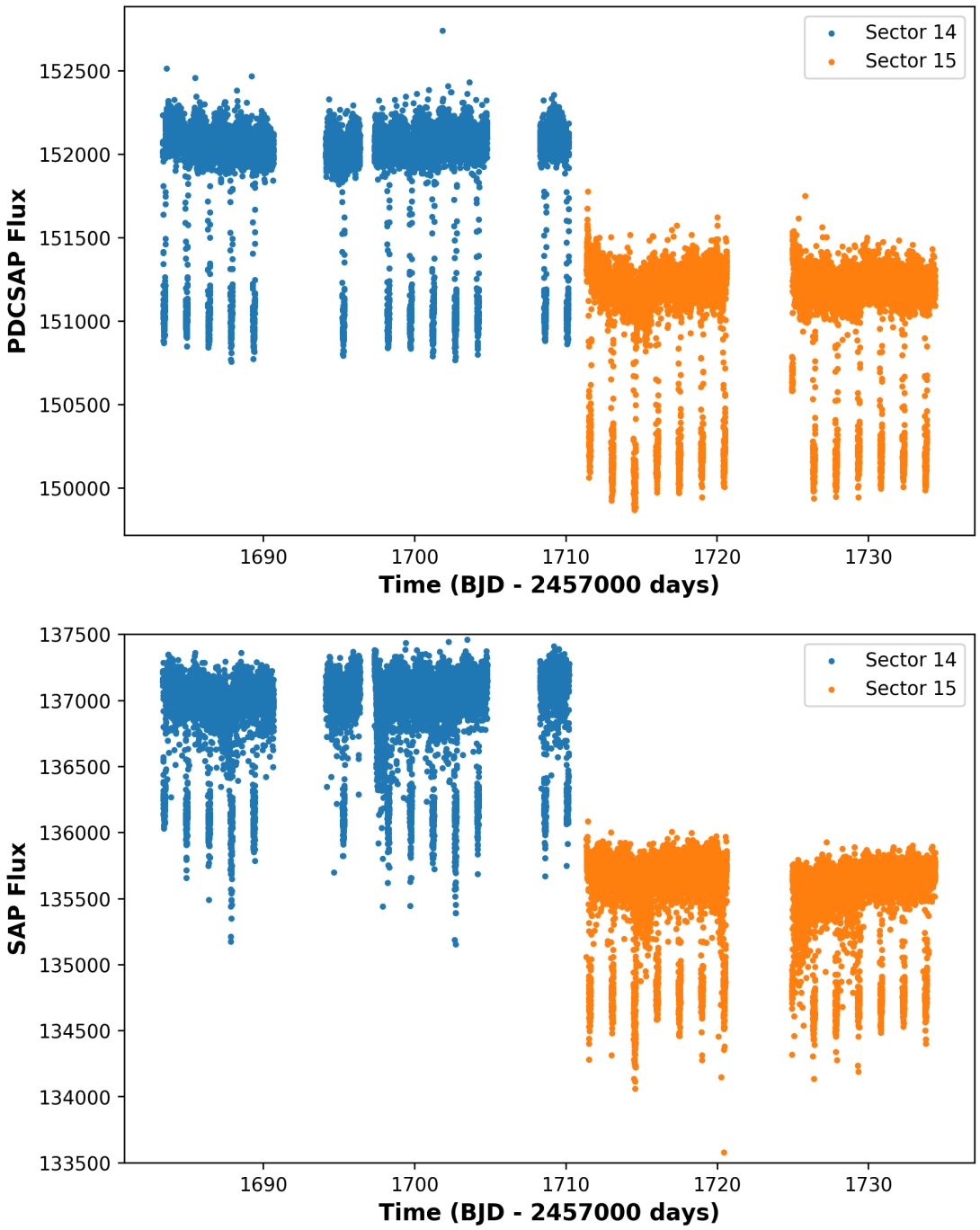

Figure 3.3 Comparison between PDCSAP (top) and SAP (bottom) light curve.

3.1.2 Spectroscopic data

Gaudi et al. (2017) used RV data from TRES with spectral resolution R = 44000. They used 104 of all 115 spectroscopic observations for either Doppler Tomography (DT) analysis and planetary orbit and mass. The data consist of 40 out-of-transit observations and 64 in-transit observations, used for different purposes. The 40 out-of-transit plus 3 selected in-transit observations are used to

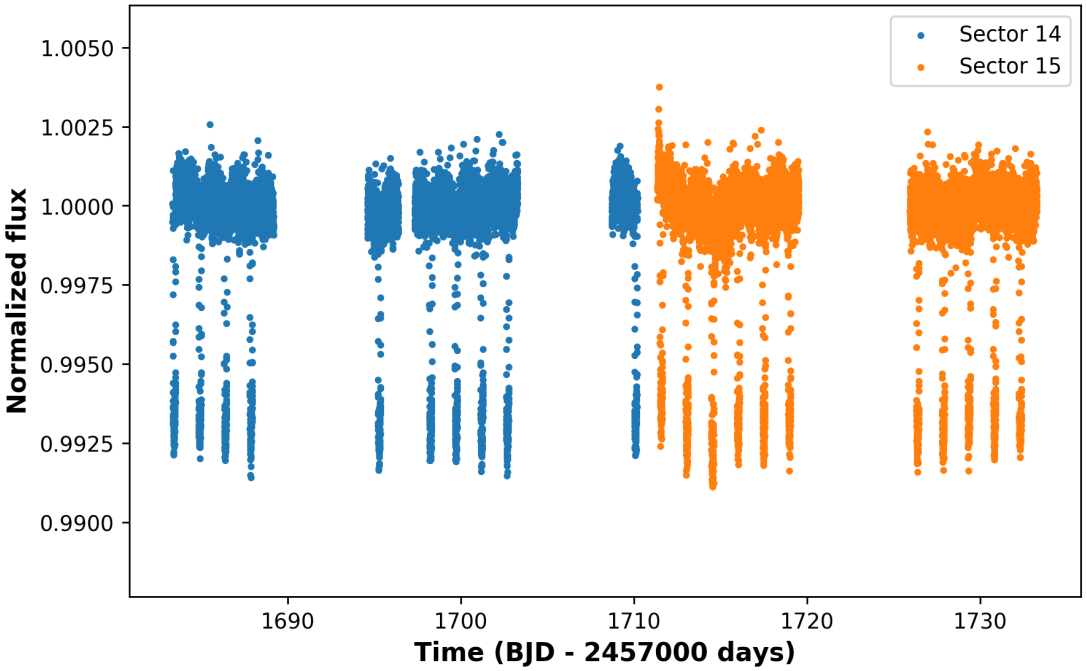

Figure 3.4 Prepared PDCSAP light curve of KELT-9.

construct planetary orbit and planet's mass, while the 64 in-transit observations, collected on 2014-11-15, 2015-11-06, and 2016-06-01 are used for doppler tomography analysis. In the spectroscopic part of this research, we obtained the 64 in-transit spectroscopic data from Gaudi et al. (2017) for our doppler tomography analysis. The spectroscopic data from 2014-11-15 are showed in Figure 3.5.

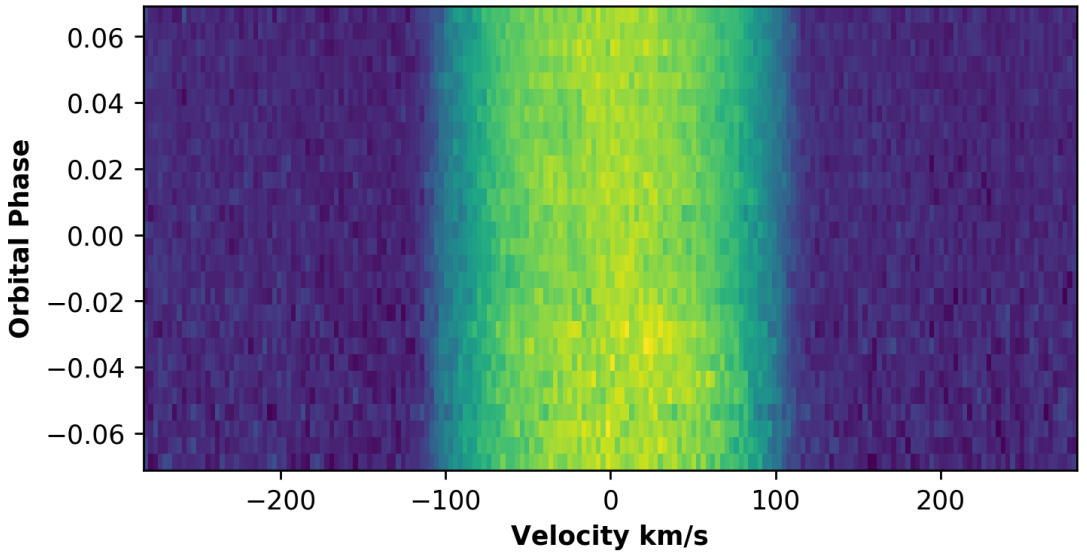

Figure 3.5 Plot of cross correlation function of radial velocity (km/s) and orbital phase from 2014-11-15.

3.1.3 Isochrone fitting data

Our isochrone fitting analysis fits the model's B, V, J, H, K, G, BP, RP band magnitude with the observed magnitude in order to constrain stellar parameters M_*, R_*, and I_{rot} which is the inclination angle of rotational axis. So, we adopt eight bands magnitude and other stellar parameters as in Table 3.1 for the analysis.

Parameters	Value	Source
Observed magnitude		
Johnson B (mag)	7.587 ± 0.130767	Mermillod
Johnson V (mag)	7.55 ± 0.01	Mermillod
J (mag)	7.458 ± 0.018	2MASS
H (mag)	7.492 ± 0.021	2MASS
K (mag)	7.482 ± 0.02	2MASS
G (mag)	7.57675 ± 0.000333	Gaia
BP (mag)	7.61109 ± 0.001626	Gaia
RP (mag)	7.56254 ± 0.002866	Gaia
Other stellar parameters		
Parallax	4.86254 ± 0.0372738	Gaia
Stellar Rotational Velocity (km· s^{-1})	111.40 ± 1.27	Gaudi et al. (2017)

Table 3.1: Stellar properties of KELT-9.

3.2 Model Creations

3.2.1 Photometric part

The phase curve variation model, including Phase function, Doppler boosting, and Ellipsoidal variation, was directly created as described in 2.2.1 (equation 2.1, 2.3, 2.4) [Also see Python code in 6]. For the secondary eclipse, we used *batman* package (Kreidberg, 2015) as our model [See equation 2.7]. Free parameters in our phase curve variation model are phase function amplitude (A_p), doppler boosting amplitude (A_d), ellipsoidal variation amplitude (A_e), and planet-to-star flux ratio (f_p). An example of our phase curve variation is shown in Figure 3.6.

Apart from phase curve variation, we include the gravity-darkening effect as described in 2.2.2 to our model. We used *simutrans* (Herman et al., 2018), which is an integrated-numerical package for gravity darkened star as our transit model. Free parameters and Python code are shown in Table 4.1 and 6 respectively. An

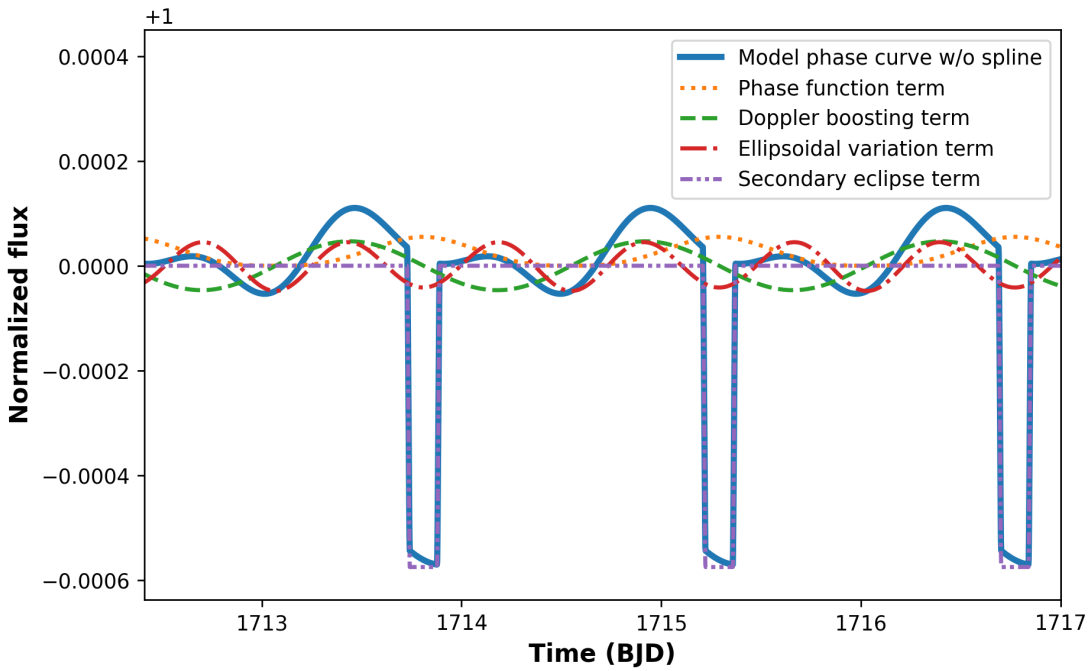

Figure 3.6 An example plot showing various components of phase curve variation model.

example of a transit light curve from *simutrans* package is shown in Figure 3.7.

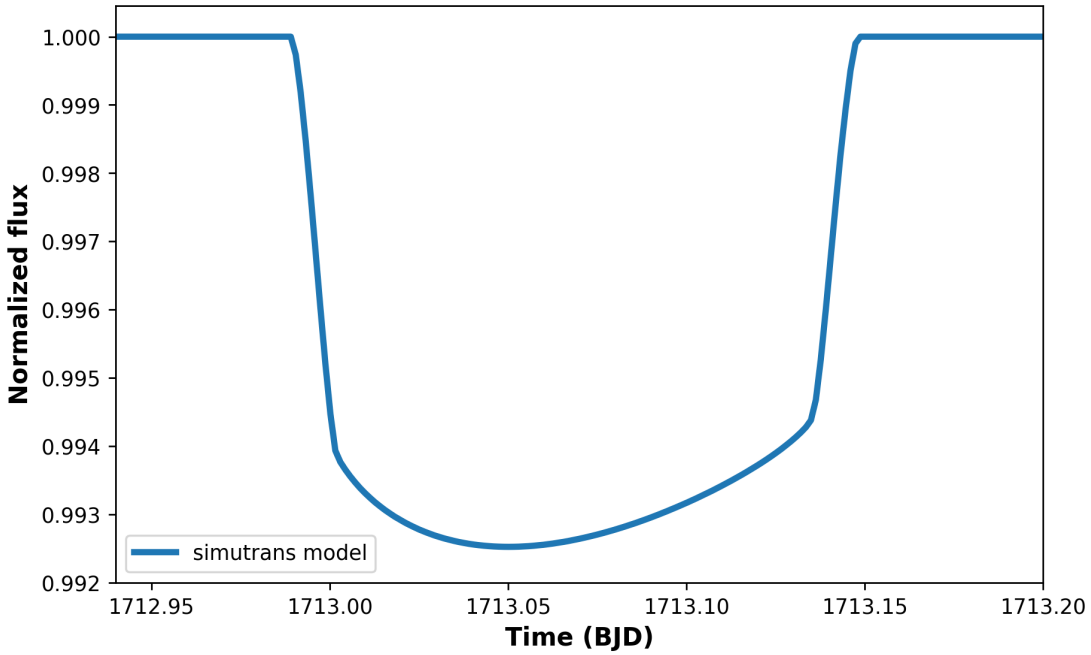

Figure 3.7 An example plot showing a gravity-darkened light curve of *simutrans* model.

In order to reduce the systematic variation, we fit for natural cubic spline separately between the sector 14 (6 knots) and 15 (8 knots) data. We assure that

this spline fitting does not affect either phase curve variation fitting and transit fitting by visualization, as showed in Figure 3.8. From the figure, we have seen that variation of the spline is much smaller than variations due to phase curve or transit.

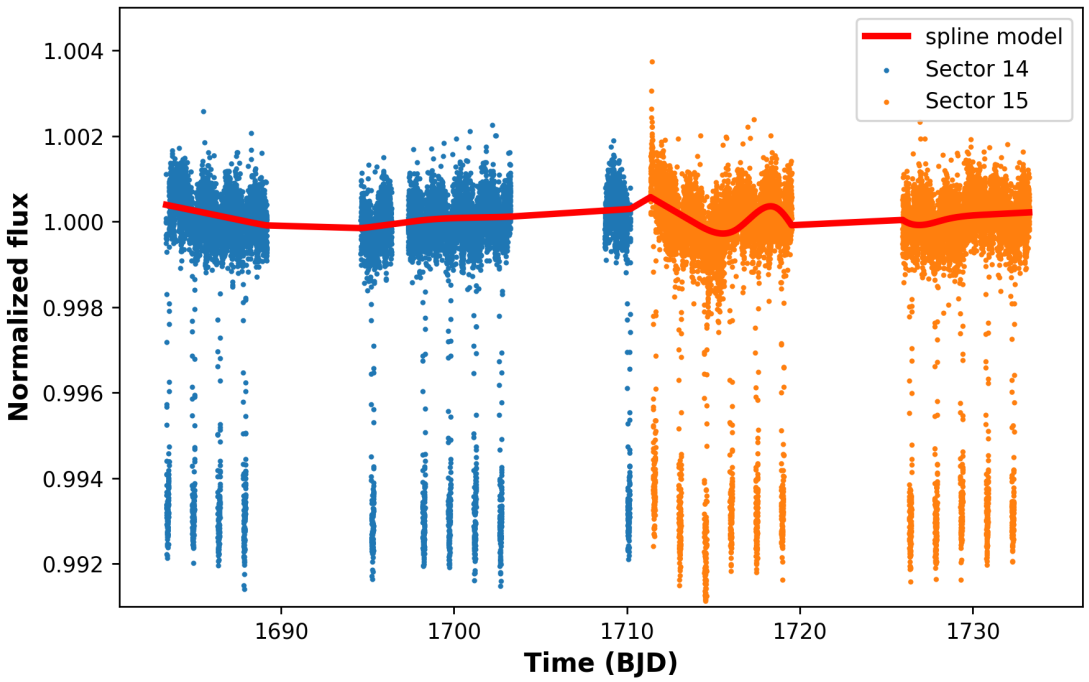

Figure 3.8 A plot of spline model over the data.

3.2.2 Spectroscopic part

For the spectroscopic part, we model our data by the novel doppler tomography technique.

Doppler tomography technique, which was used in Zhou et al. (2019), Collier Cameron et al. (2010) etc., is a spectroscopic technique using the Rossiter–McLaughlin (RM) effect [See 2.3.1] to determine the sky-projected spin-orbit misalignment angle (λ). This technique also needs a transit model to construct a shadow of the planet. After modeling the transit, we then perform calculation of the stellar rotational velocity part by cross-correlating the target star spectrum with a standard star spectrum. The width of the cross-correlation function (also refer to the width of the matching spectral line) is interpreted as stellar rotational velocity.

Using the rotational velocity of v_{rot} = 111.4 km/s from Gaudi et al. (2017), we can create the model of cross-correlation function. Then, we combine transit

model and cross-correlation function together to construct the doppler tomography model as in Figure 3.9.

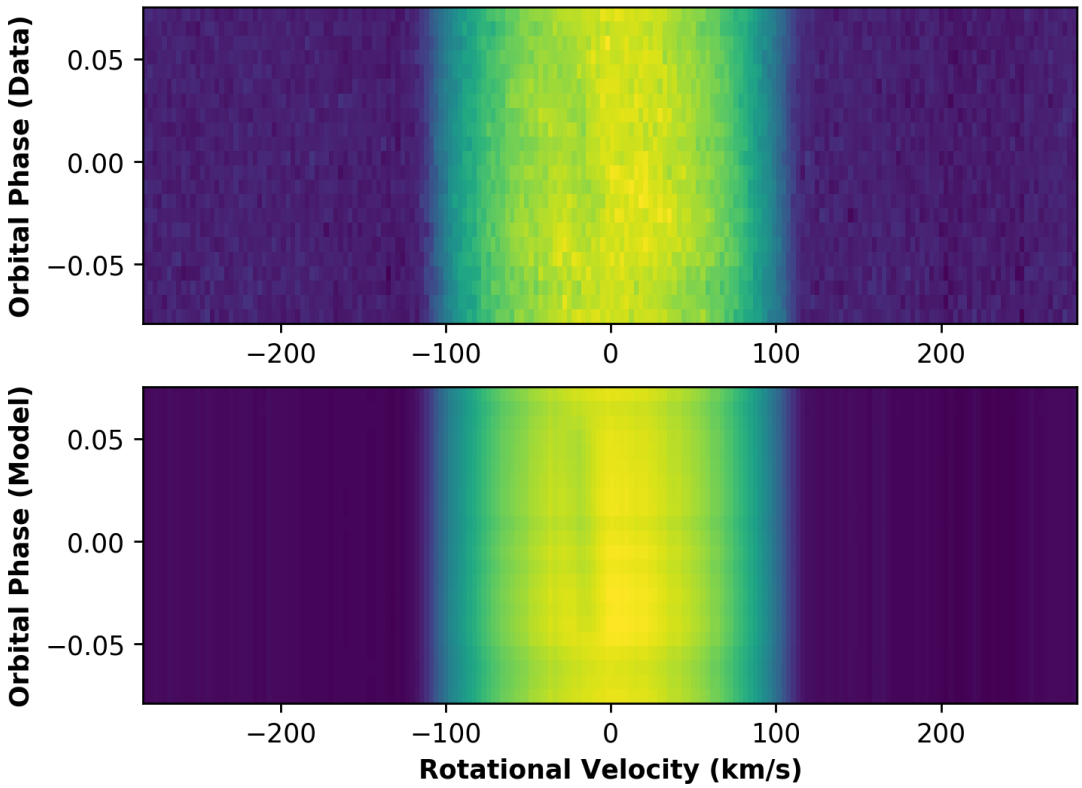

Figure 3.9 An example of spectroscopic data (top) and Doppler Tomography model (bottom).

3.2.3 Isochrone fitting part

For isochrone fitting, we used the mass (m_{star}) and radius (r_{star}) (both are free parameter), rotational angle (I_{rot}) (free parameter), rotational velocity (v_{rot}) (fixed at 111.4 km/s), and parallax angle (fixed at 4.8625') of host star as parameters. We used those parameters to determine the expected band magnitude. Then, we use the observed band magnitudes data in 3.1 to fit and give the log-likelihood function and stellar oblateness due to high rotational velocity for each model (respected to set of inserted parameters).

3.3 Analysis Calculation

A Markov chain Monte Carlo (MCMC) algorithm (Goodman and Weare, 2010) is a usual approach in astrophysics to determine the posterior distribution of parameter space. The posterior distribution $P(\theta|D, M)$ can be simply represented as in equation 3.1

$$P(\theta|D, M) \propto P(D|\theta, M)P(\theta|M), \tag{3.1}$$

where
$P(\theta|D, M)$ is the posterior distribution of parameter θ after given Model (M) and Data (D),
$P(D|\theta, M)$ is the likelihood function, and
$P(\theta|M)$ is the prior (An initial guess about the parameter).

After we let MCMC run, each walker will explore our parameter space and finally walk to the maximum and create a posterior distribution.

In this research, we used the Python-based affine-invariant Markov Chain Monte Carlo package, named *emcee* (Foreman-Mackey et al., 2013) to get the posterior distribution. We found that our algorithm needs higher computational resources than a single computer. So, we ran our code in the galaxy cluster, which is a local cluster in astrophysics lab at the Department of Physics, Mahidol University.

Chapter 4

Results and Discussion

After running MCMC through gravity darkening included model, we got a posterior distribution of each parameter shown in Figure 4.1. Figure 4.1 is produced by *corner* Python package (Foreman-Mackey, 2016). The histogram at the top of each column is a posterior distribution of one specific parameter, while the other plots in the column is the covariance between each pair of parameters. Most parameters are distributed as gaussian except M_*, R_*, and I_{rot}, which are parameters in the isochrone fitting part. The reason for that will be discussed in 4.3

Median values and 2σ errors of parameters from gravity-darkening included model (*simutrans* package) are listed in Table 4.1 along with no-gravity darkening included model (*batman* package) and Gaudi et al. (2017).

4.1 Photometric results

From the table, we pointed out the difference in R_p/R_*. The difference is directly from the gravity darkening effect. In this case, the planet transit blocked the brighter part of the star (pole). So, we shall get R_p/R_* larger than it actually be, if gravity darkening effect is not taken into account. We indicated the significant different (over 1σ) from $0.079772^{+0.000059}_{-0.000061}$ and $0.081094\ ^{+0.000077}_{-0.000079}$ from models with and without gravity darkening effect. Moreover, as we mention in 2.2.2, we now can fit for stellar rotation angle $I_{rot} = 58.67\ ^{+0.88}_{-0.34}$ degree in order to understand more about the stellar configuration.

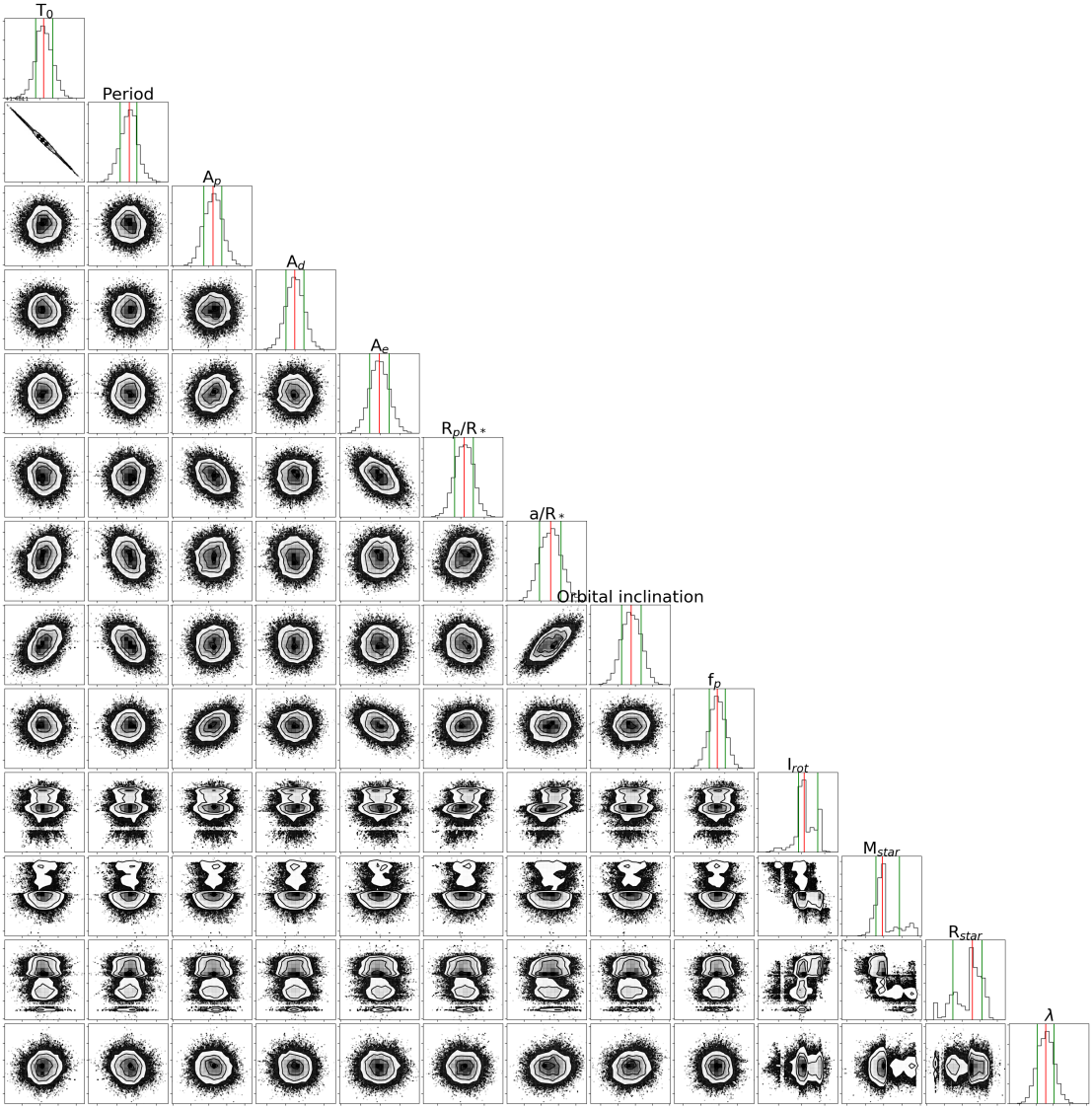

Figure 4.1 A corner plot of posterior distributions from MCMC.

A plot of models with and without gravity darkening effect is shown in Figure 4.2. The model with gravity darkening shows a better fit, especially during transit, as we expected.

Finally, we also compare our phase curve variation fitting model with Wong et al. (2019) approach, which used an nth-order Fourier series at phase ϕ instead of combining each physical effect like ours. We decided to illustrate the difference between our phase curve model and Wong et al. (2019) model in Figure 4.3. Instead of using all parameters calculated in Wong et al. (2019), we ran MCMC through Wong et al. (2019)'s model to get a better fit in our configuration i.e., data masking, spline fitting. The plots show a better fit in Wong et al. (2019)'s work due to a more empirical model. However, our phase curve model followed Esteves

Parameters	Model with G-Dark	Model without G-Dark	Gaudi et al. (2017)
Transit parameters			
T_0 (days - 2457000)	$95.6830\ ^{+0.0013}_{-0.0011}$	$95.6751\ ^{+0.0033}_{-0.0034}$	95.68572 ± 0.00014
Period (days)	$1.48112156\ ^{+0.00000098}_{-0.00000114}$	$1.4811286\ ^{+0.0000031}_{-0.0000030}$	1.4811235 ± 0.0000011
R_p/R_*	$0.079772\ ^{+0.000059}_{-0.000061}$	$0.081094\ ^{+0.000077}_{-0.000079}$	0.08228 ± 0.00043
a/R_*	$3.1430\ ^{+0.0031}_{-0.0032}$	3.100 ± 0.016	3.153 ± 0.011
i_{orb} (deg)	$86.678\ ^{+0.058}_{-0.056}$	$84.41\ ^{+0.37}_{-0.34}$	86.79 ± 0.25
e	0.0 (fixed)	0.0 (fixed)	0.0 (fixed)
ω_*	90.0 (fixed)	90.0 (fixed)	90.0 (fixed)
Phase curve parameters			
A_p (ppm)	$498.7\ ^{+7.3}_{-8.0}$	$496.3\ ^{+7.6}_{-7.4}$	-
A_d (ppm)	$44.9\ ^{+2.9}_{-2.8}$	49.9 ± 2.9	-
A_e (ppm)	$23.8\ ^{+4.0}_{-3.9}$	24.4 ± 4.0	-
f_p (ppm)	$637.2\ ^{+9.0}_{-8.9}$	639.8 ± 8.9	-
Stellar parameters			
I_{rot} (deg)	$58.67\ ^{+0.88}_{-0.34}$	-	-
M_{star} ($M_\odot$)	$2.52\ ^{+0.056}_{-0.020}$	-	$2.52\ ^{+0.25}_{-0.20}$
R_{star} ($R_\odot$)	$2.147\ ^{+0.016}_{-0.033}$	-	$2.362\ ^{+0.075}_{-0.063}$
λ (deg)	274.78 ± 0.25	-	275.2 ± 1.4
vsini (km/s)	111.4 ± 1.3 (adopt)	-	111.4 ± 1.3 (this work)

Table 4.1: Parameters' median and 1σ error.

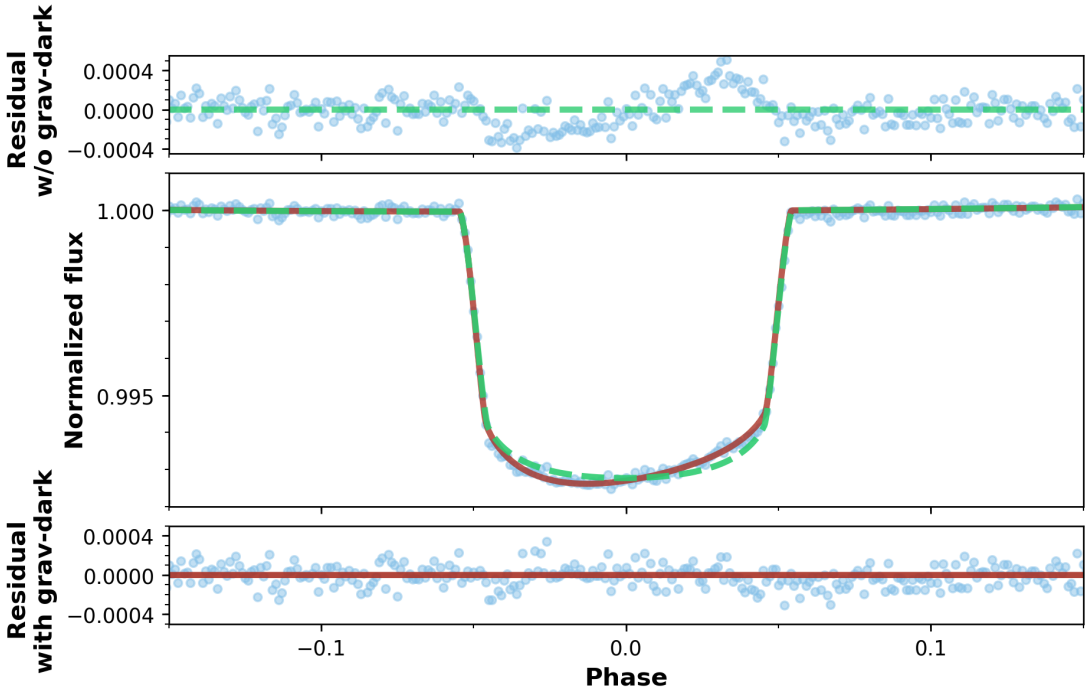

Figure 4.2 A plot of two models with and without gravity darkening effect.

et al. (2013) can be understood better in term of underlying physical effects.

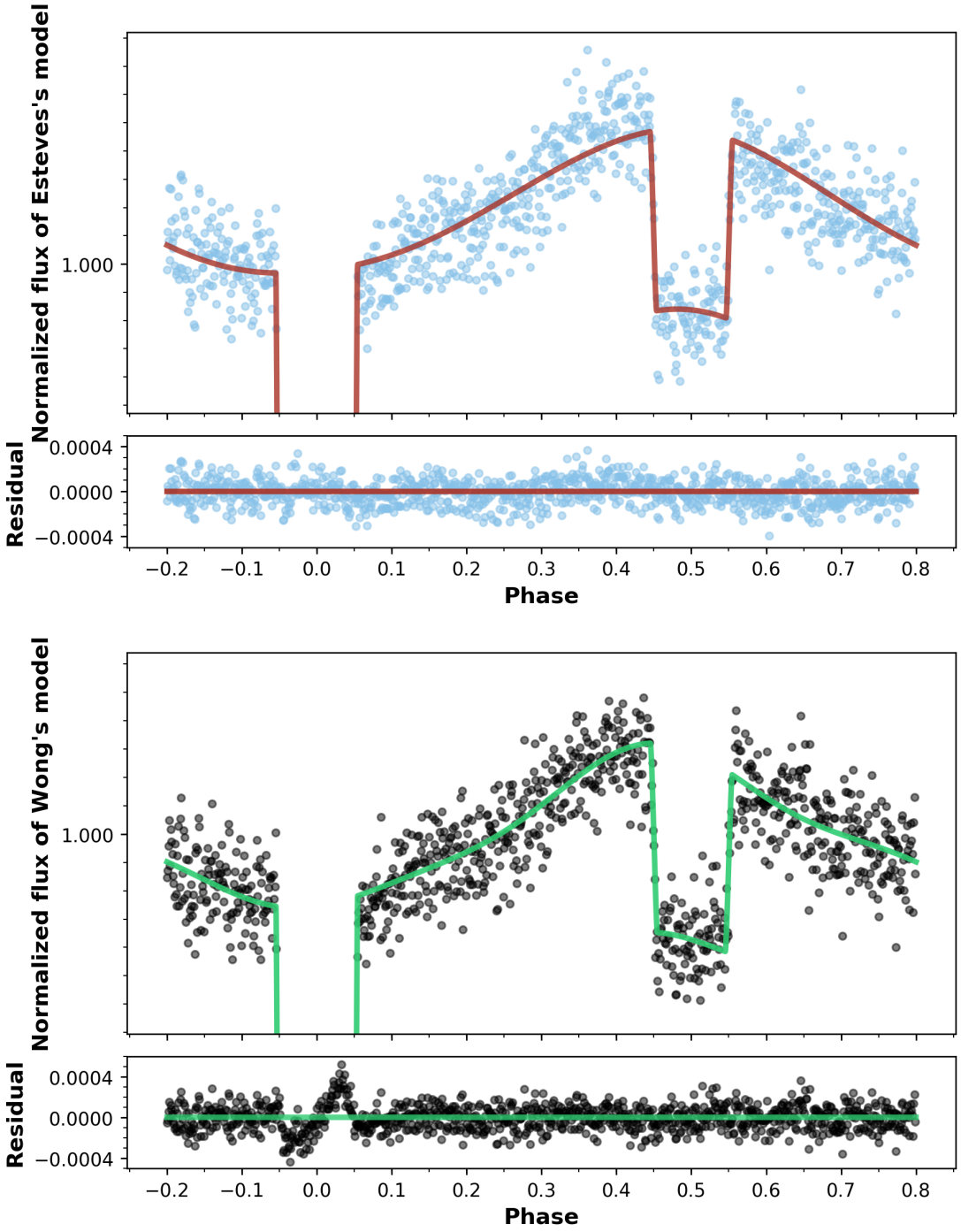

Figure 4.3 A plot of two phase curve variation models, Esteves et al. (2013)'s model, and Wong et al. (2019)'s model.

4.2 Spectroscopic results

As we mentioned in 3.2.2 that we included a spectroscopic part for constraining the sky-projected spin-orbit misalignment angle (λ) more precisely. The contour plot of 3-days in-transit spectroscopic data, model, and residual are shown

in Figure 4.4 top, middle, and bottom panel respectively. We can see that our best-fit parameters allow the model to fit the data correctly with no significant structure in residual. It also helps in fitting $\lambda = 274.78 \pm 0.25$ degree which we can compare that we got the significantly lower error in λ.

4.3 Isochrone results

Isochrone fitting in our model aimed to fit for stellar parameters such as M_{star}, R_{star}, I_{rot}, etc. The process and data for isochrone fitting are described in 3.2.3. The plot of the model's and data's apparent magnitudes is shown in Figure 4.5. As in Figure 4.5, we cannot perfectly fit the data. The reason behind this is the same reason that the posterior distribution of stellar parameters in 4.1 is not in perfect gaussian. It directly comes from our model that we cannot properly interpolate the isochrone since they are sparsely sampled. We deal with this problem by taking the 68-percentile range of posterior distribution (especially in stellar parameters) in our result.

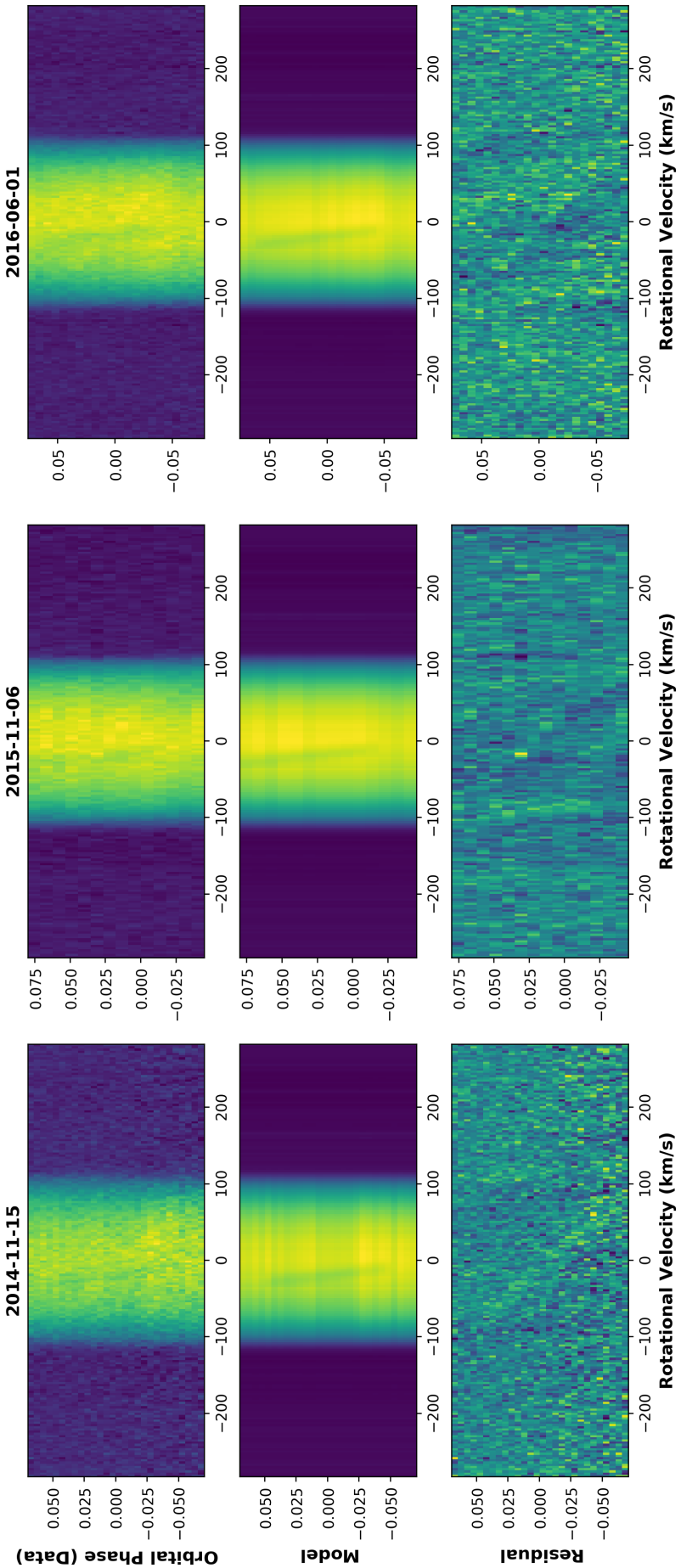

Figure 4.4 A contour plot of 3-days in-transit spectroscopic data (Top), model (Middle), and residual (Bottom).

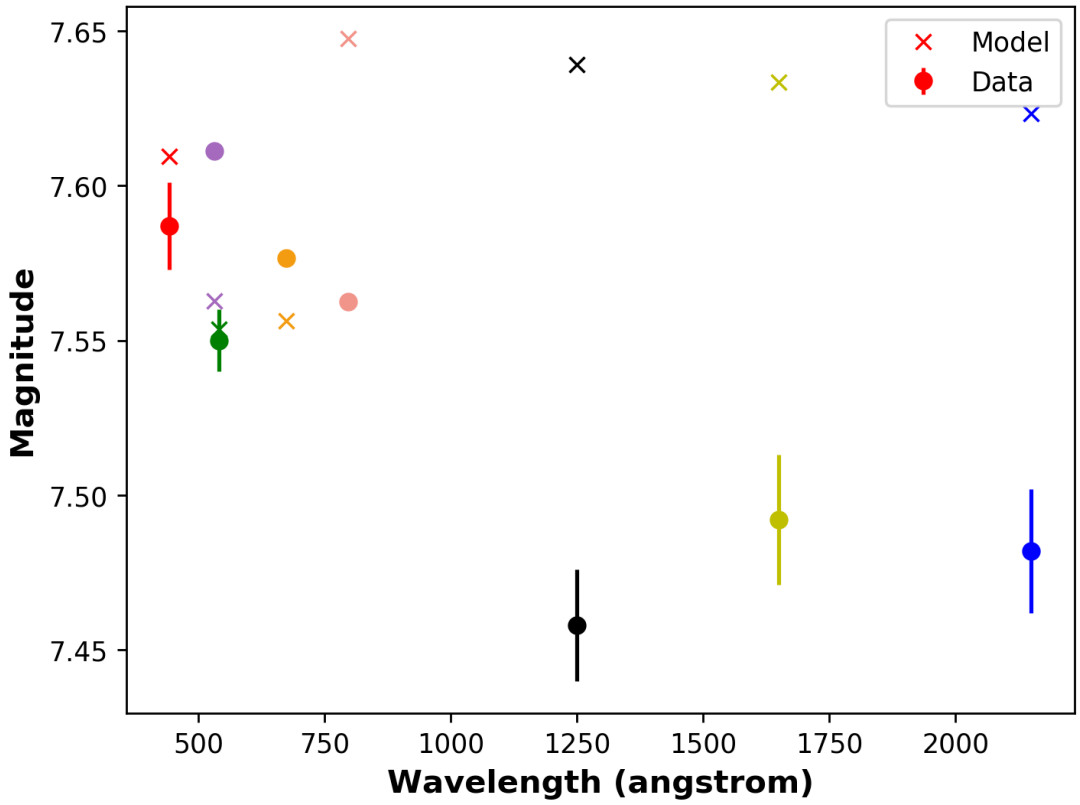

Figure 4.5 A plot of apparent magnitude in different bandpass filters.

Chapter 5

Conclusions

This research primarily aims to study phase curve variation and gravity-darkened transit, which is a photometric effects. Parameter values calculated from 68-percentile from the posterior distribution of Markov-Chain Monte-Carlo (MCMC, *emcee*), as showed in Table 4.1, are all in reasonable agreements with each other. We also include the Doppler tomography technique and isochrone fitting to help constrain λ and stellar parameters, respectively. Finally, we need to point out the importance and the potential of TESS to detect gravity-darkened transit and also phase curve variation to understand the physics of exoplanet systems better.

References

Albrecht, S. et al. (Sept. 2012). "Obliquities of Hot Jupiter Host Stars: Evidence for Tidal Interactions and Primordial Misalignments". In: 757.1, 18, p. 18.

Barnes, J. W. (Nov. 2009). "Transit Lightcurves of Extrasolar Planets Orbiting Rapidly Rotating Stars". In: 705.1, pp. 683–692.

Barnes, J. W., E. Linscott, and A. Shporer (Nov. 2011). "Measurement of the Spin-Orbit Misalignment of KOI-13.01 from Its Gravity-darkened Kepler Transit Lightcurve". In: 197.1, 10, p. 10.

Collier Cameron, A. et al. (Mar. 2010). "Line-profile tomography of exoplanet transits - I. The Doppler shadow of HD 189733b". In: 403.1, pp. 151–158.

Espinosa Lara, F. and M. Rieutord (Sept. 2011). "Gravity darkening in rotating stars". In: 533, A43, A43.

Esteves, L. J., E. J. W. De Mooij, and R. Jayawardhana (July 2013). "Optical Phase Curves of Kepler Exoplanets". In: 772.1, 51, p. 51.

Foreman-Mackey, D. (June 2016). "corner.py: Scatterplot matrices in Python". In: *The Journal of Open Source Software* 1, p. 24.

Foreman-Mackey, D. et al. (Mar. 2013). "emcee: The MCMC Hammer". In: 125.925, p. 306.

Gaudi, B. S. et al. (June 2017). "A giant planet undergoing extreme-ultraviolet irradiation by its hot massive-star host". In: 546.7659, pp. 514–518.

Goodman, J. and J. Weare (Jan. 2010). "Ensemble samplers with affine invariance". In: *Communications in Applied Mathematics and Computational Science* 5.1, pp. 65–80.

Herman, M. K. et al. (Jan. 2018). "Spin-Orbit Misalignment and Precession in the Kepler-13Ab Planetary System". In: 155.1, 13, p. 13.

Jenkins, J. M. et al. (2016). "The TESS science processing operations center". In: vol. 9913. Society of Photo-Optical Instrumentation Engineers (SPIE) Conference Series, 99133E.

Kreidberg, L. (Nov. 2015). "batman: BAsic Transit Model cAlculatioN in Python". In: 127.957, p. 1161.

Mayor, M. and D. Queloz (Nov. 1995). "A Jupiter-mass companion to a solar-type star". In: 378.6555, pp. 355–359.

McLaughlin, D. B. (July 1924). "Some results of a spectrographic study of the Algol system." In: 60, pp. 22–31.

Morris, S. L. (Aug. 1985). "The ellipsoidal variable stars." In: 295, pp. 143–152.

Rossiter, R. A. (July 1924). "On the detection of an effect of rotation during eclipse in the velocity of the brigher component of beta Lyrae, and on the constancy of velocity of this system." In: 60, pp. 15–21.

Russell, H. N. (Apr. 1916). "On the Albedo of the Planets and Their Satellites". In: 43, pp. 173–196.

Shporer, A. et al. (May 2019). "TESS Full Orbital Phase Curve of the WASP-18b System". In: 157.5, 178, p. 178.

Smith, J. C. et al. (Sept. 2012). "Kepler Presearch Data Conditioning II - A Bayesian Approach to Systematic Error Correction". In: 124.919, p. 1000.

Stumpe, M. C., J. C. Smith, J. H. Catanzarite, et al. (Jan. 2014). "Multiscale Systematic Error Correction via Wavelet-Based Bandsplitting in Kepler Data". In: 126.935, p. 100.

Stumpe, M. C., J. C. Smith, J. E. Van Cleve, et al. (Sept. 2012). "Kepler Presearch Data Conditioning I—Architecture and Algorithms for Error Correction in Kepler Light Curves". In: 124.919, p. 985.

Szabó, G. M. et al. (July 2011). "Asymmetric Transit Curves as Indication of Orbital Obliquity: Clues from the Late-type Dwarf Companion in KOI-13". In: 736.1, L4, p. L4.

von Zeipel, H. (June 1924). "The radiative equilibrium of a rotating system of gaseous masses". In: 84, pp. 665–683.

Wong, I. et al. (Oct. 2019). "Exploring the atmospheric dynamics of the extreme ultra-hot Jupiter KELT-9b using TESS photometry". In: *arXiv e-prints*, arXiv:1910.01607, arXiv:1910.01607.

Zhou, G. et al. (Jan. 2019). "HATS-70b: A 13 MJ Brown Dwarf Transiting an A Star". In: 157.1, 31, p. 31.

Chapter 6

Appendix

```
#!/usr/bin/env python2
# -*- coding: utf-8 -*-
"""
Created on Wed Jun 26 11:56:44 2019

@author: patcharapol
"""

import numpy as np
import matplotlib.pyplot as plt
import time,os,sys,pickle
import get_natural_spline
from fitiso import isochrone_lnlike

sys.path.append("simuTrans-noprecession")
from transit import model as transitmodel
import DT_function
sys.path.append('/work/patch/site-package-patch/lib/
    ↪ python2.7/site-packages')
import emcee
from emcee.utils import MPIPool
import batman



def model(theta,data,oblateness,vsini,beta,return_spline=
    ↪ False,sep_model=False,fratio_need=False,plot=False):
    t0,per,a,b,c,rprs,ars,inc,fp,irot,m_star,r_star,lam =
        ↪ theta
    ## data ##
    data_all = np.concatenate((data[0],data[1]),axis=1)
    x = data_all[0]
    y = data_all[1]


    ## Transit parameter ##
    t0 = t0
```

```
    per =  per
    beta = beta
    lam = lam
    ecc =  0.
    w = 90.0
    u1 = 0.1588
    u2 = 0.2544


    ## Phase calculation ##
    phase = (x-t0)/per
    phase = phase-np.floor(phase)
    phase[phase>0.8] = phase[phase>0.8]-1.0

    ## Primary and secondary transit mask ##
    mask_prim = ((phase>=-0.15) & (phase<=0.15))
    phase_transit = phase[mask_prim]
    mask_sec = ((phase>=0.3) & (phase<=0.7))
    t = x[mask_sec]

    i=(inc*np.pi)/180 #orbital inclination in radian
    ### Phase curve variation ###
    z = np.arccos(-np.sin(i)*np.cos(2*np.pi*phase))
    F_p = a*((np.sin(z)+(np.pi-z)*np.cos(z))/np.pi) ##
       ↪ Phase Function##
    F_d = b*np.sin(2*np.pi*phase)## Doppler Boosting ##
        ### Ellipsoidal Variations ###
    alpha1 = ((25*u1)/(24*(15+u1)))*((u2+2)/(u2+1))
    f1 = 3*alpha1*(ars)**(-1)*((5*(np.sin(i))**2 - 4)/(np.
       ↪ sin(i)))
    f2 = 5*alpha1*(ars)**(-1)*(np.sin(i))
    F_e = -c*(np.cos(2*np.pi*2*phase)+f1*np.cos(2*np.pi*
       ↪ phase)+f2*np.cos(2*np.pi*3*phase))

    #### Transit model ####
    irot=irot
    ld1 = u1 ### limb darkening coeff 1 -- keep this fixed
    ld2 = u2 ### limb darkening coeff 2 -- keep this fixed
    fratio = oblateness ### Rpole/Requator for the star --
       ↪  keep this fixed
    beta = beta ### gravity darkening coefficient, keep
       ↪ this fixed
    lam = lam### projected obliquity, take this from
       ↪ discovery paper as a prior
    mstar = m_star ### stellar mass, fix this from
       ↪ discovery paper
    Req = r_star# ### stellar radius at equator, fix this
       ↪ from discovery paper
    vsini = vsini# ### vsini, fix this from discovery
       ↪ paper
    impact_b = ars*np.cos(i)
```

```
77      transit_model_input = [1000,ld1,ld2,fratio,irot,0,beta
           ↪ ,500,impact_b,rprs,ars,lam,0,mstar,Req,vsini/np.
           ↪ sin(irot*np.pi/180.)]
78      lcmodel = (transitmodel(phase_transit,
           ↪ transit_model_input))
79      transit_model = np.ones(len(phase))
80      transit_model[mask_prim] = lcmodel
81      ### Plot fot transit ###
82      # plt.scatter(phase[mask_prim],y[mask_prim],s=4)
83      # plt.plot(phase_transit,lcmodel,'.r')
84      # plt.show()
85
86
87      #####Secondary eclipse model #######
88      params = batman.TransitParams()
89      t0 = t0
90      period = per
91      params.per = period
92      params.fp = fp
93      params.limb_dark = "quadratic"
94      params.u = [u1,u2]
95      params.rp = rprs
96      params.a = ars
97      params.inc = inc
98      params.ecc = ecc#
99      params.w = w#
100     params.t_secondary = (t0-(period/2.))
101
102     sec_model = np.ones(len(phase))
103     m = batman.TransitModel(params, t, transittype="
           ↪ secondary")
104     seclipse_model = m.light_curve(params)-fp
105
106     sec_model[mask_sec] = seclipse_model
107
108     ##### Final model #####
109     model = (F_p+F_d+F_e+1)*transit_model*sec_model
110
111     ## Fit for spline ##
112     x14 = data[0][0]
113     x15 = data[1][0]
114
115     res = y-model
116     s14 = get_natural_spline.
           ↪ get_natural_cubic_spline_model(x14, res[x<=max(
           ↪ x14)], minval=min(x14), maxval=max(x14), n_knots
           ↪ =6)
117     s14 = s14.predict(x14)
118
119
```

```
120     s15 = get_natural_spline.
           ↪ get_natural_cubic_spline_model(x15, res[x>max(x14
           ↪ )], minval=min(x15), maxval=max(x15), n_knots=8)
121     s15 = s15.predict(x15)
122
123     s = np.concatenate((s14,s15))
124
125     if plot:
126         plt.scatter(x,y)
127         plt.plot(x,model+s,'.r')
128         plt.plot(x,s+1,'-b')
129         plt.show()
130 #     sys.exit()
131
132     model = model+s
133
134     if return_spline:
135         return model,s
136     else:
137         if sep_model:
138             return F_p,F_d,F_e
139         else:
140             if fratio_need:
141                 return model,fratio
142             else: return model
143
144
145 def log_prior(theta):
146     t0,per,a,b,c,rprs,ars,inc,fp,irot,m_star,r_star,lam =
           ↪ theta
147     b_inc = ars * np.cos((inc*np.pi)/180)
148     if (200.0 < lam < 300.0) and (1.0>rprs>0.0) and (3.5>
           ↪ ars>2.0) and (b_inc<1.0) and (110.0 > inc > 80.0)
           ↪  and (a>0.0)and (b>0.0)and (c>0.0) and (m_star>0)
           ↪  and (r_star>0):
149         #print theta
150         return 0.0
151     else :
152
153         return -np.inf
154
155
156 def lnlike(theta,data,return_obnvsin = False,plot=False):
157     t0,per,a,b,c,rprs,ars,inc,fp,irot,m_star,r_star,lam =
           ↪ theta
158     parallax = 4.8625
159     vsini = 111.4 ### km/s
160     beta = 0.24
161
162     ### Isochrone ###
```

```
163     observed_mags = np.genfromtxt("gravdark_isochrone/
            ↪ observed_mags",invalid_raise=False)
164     theta_sm = [m_star,r_star,irot]
165     lnlike_star,oblateness = isochrone_lnlike(theta_sm,
            ↪ observed_mags,parallax,vsini)
166
167     m,fratio = model(theta,data,oblateness,vsini,beta,
            ↪ fratio_need=True,plot=plot)
168     # print 'fratio',fratio
169     data_all = np.concatenate((data[0],data[1]),axis=1)
170     x = data_all[0]
171     y = data_all[1]
172     yerr = data_all[2]
173
174     chisq1 = np.sum(((m-y)/yerr)**2)
175
176     lnlike_dt = DT_function.run_doppler(t0,per,rprs,ars,
            ↪ inc,lam,irot,m_star,r_star,vsini,beta,fratio,plot
            ↪ =plot)
177
178     lnlike_all = (-0.5*chisq1) + lnlike_star  + lnlike_dt
179     print 'lnlike simutrans',lnlike_all
180     if return_obnvsin:
181         return oblateness,vsini
182     else:
183         return lnlike_all
184
185 def log_prob(theta,data,plot=False):
186     t0,per,a,b,c,rprs,ars,inc,fp,irot,m_star,r_star,lam =
            ↪ theta
187     lp = log_prior(theta)
188
189     lnlike_model = lnlike(theta,data,plot=plot)
190
191     if not np.isfinite(lp):
192         return -np.inf
193     else :
194         return lp + lnlike_model
195
196 if __name__ == "__main__":
197     data14 = pickle.load(open('data_KELT9_short_PDC_14.pkl
            ↪ ','rb'))
198     data15 = pickle.load(open('data_KELT9_short_PDC_15.pkl
            ↪ ','rb'))
199
200     ##Mask weird transit out##
201     ## Only for sector 15 included ###
202     index1 = (data15[0]<1724.93585)
203     index2 = (data15[0]>1725.94321225)
204
205     data15[0] = data15[0][index1 | index2]
```

```
206     data15[1] = data15[1][index1 | index2]
207     data15[2] = data15[2][index1 | index2]
208     data = [data14 , data15]
209
210
211     ###Constant###
212     nwalkers = 100
213     start_point = []
214
215     ### Initialized starting point ###
216     with MPIPool() as pool:
217         if not pool.is_master():
218             pool.wait()
219             sys.exit(0)
220
221         ndim = len(start_point)
222
223         print 'Result from minimize ...',start_point
224
225         pos = np.zeros((nwalkers,len(start_point)))
226
227         n = 0
228         sd_start = []
229         while True:
230             n = n+1
231             print 'Round',n
232             for k in range(nwalkers):
233                 for j in range(0,len(start_point)):
234                     pos[k][j] = np.random.normal(
                            ↪ start_point[j],sd_start[j]) ##
235
236             logprob=np.zeros(len(pos))
237             okay = np.zeros(len(pos))
238             for p in range(len(pos)):
239                 logprob[p]=log_prob(pos[p],data,plot=True)
240                 print logprob[p]
241             okay = (~np.isnan(logprob)) * (logprob != -1*
                    ↪ np.inf)
242             print (pos[okay==False])
243             if all(okay) == True:
244                 print 'Got that!!!'
245                 print okay
246                 print logprob
247
248                 break
249
250
251
252         sampler = emcee.EnsembleSampler(nwalkers, ndim,
                ↪ log_prob,pool=pool,args=[data])
253
```

```
254
255         print 'Burning-in...'
256         t0 = time.time()
257         pos, prob, state = sampler.run_mcmc(pos,2000)
258         t1 = time.time()
259         total = t1-t0
260         print total
261         chain_burn = sampler.chain
262         pickle.dump(chain_burn,open('
               ↪ chain_KELT9_burn_proj_1.pkl','wb'))
263
264         sampler.reset()
265
266         print 'Running MCMC...'
267         t2 = time.time()
268         sampler.run_mcmc(pos, 4000)
269         t3 = time.time()
270         total_run = t3-t2
271         print total_run
272         chain = sampler.chain
273         print chain
274         pickle.dump(chain,open('chain_KELT9_all_proj_1.pkl
               ↪ ','wb'))
275         pool.close()
```